Developmental Cell
Short Article

# Nodal Signaling Range Is Regulated by Proprotein Convertase-Mediated Maturation

Federico Tessadori,[1] Emily S. Noël,[1] Elisabeth G. Rens,[2,3] Roberto Magliozzi,[1] Inkie J.A. Evers-van Gogh,[1,4] Daniele Guardavaccaro,[1] Roeland M.H. Merks,[2,3] and Jeroen Bakkers[1,*]
[1]Cardiac Development and Genetics, Hubrecht Institute-KNAW and University Medical Centre Utrecht, 3584 CT Utrecht, the Netherlands
[2]Life Sciences Group, Centrum Wiskunde and Informatica, 1098 XG Amsterdam, the Netherlands
[3]Mathematical Institute, Leiden University, 2333 CA Leiden, the Netherlands
[4]Present address: Molecular Cancer Research, Section Metabolic Diseases, University Medical Centre Utrecht, 3584 EA Utrecht, the Netherlands
*Correspondence: j.bakkers@hubrecht.eu
http://dx.doi.org/10.1016/j.devcel.2014.12.014

## SUMMARY

**Tissue patterning is established by extracellular growth factors or morphogens. Although different theoretical models explaining specific patterns have been proposed, our understanding of tissue pattern establishment in vivo remains limited. In many animal species, left-right patterning is governed by a reaction-diffusion system relying on the different diffusivity of an activator, Nodal, and an inhibitor, Lefty. In a genetic screen, we identified a zebrafish loss-of-function mutant for the proprotein convertase FurinA. Embryological and biochemical experiments demonstrate that cleavage of the Nodal-related Spaw proprotein into a mature form by FurinA is required for Spaw gradient formation and activation of Nodal signaling. We demonstrate that FurinA is required cell-autonomously for the long-range signaling activity of Spaw and no other Nodal-related factors. Combined in silico and in vivo approaches support a model in which FurinA controls the signaling range of Spaw by cleaving its proprotein into a mature, extracellular form, consequently regulating left-right patterning.**

## INTRODUCTION

Theoretical and experimental work have proposed and validated mechanisms for establishing morphogen gradients (Müller et al., 2013; Wartlick et al., 2009). Most models assume diffusive transportation of the signaling protein or mRNA from a localized source. For example, the synthesis, diffusion, degradation model, originally proposed to explain the exponentially decaying gradient of Bicoid in *Drosophila* zygotes (Driever and Nüsslein-Volhard, 1988), assumes diffusion of the morphogen from a localized synthesis site and first-order degradation, forming an exponential gradient in steady state. Variants of this model include fine-tuning or stabilization of the gradient through binding to receptors or the extracellular matrix (reviewed in Müller et al., 2013).

During somitogenesis, the vertebrate left-right (LR) axis is patterned by the interplay of Nodal and its repressor Lefty (reviewed in Schier, 2009; Shiratori and Hamada, 2006). Nodal expression is restricted by Lefty to the left lateral plate mesoderm (LPM), where Nodal induces its own expression in a tightly timed, forward-expanding manner. Nodal is an extracellular protein that acts at different ranges from its source and requires interaction with receptors and coreceptors to phosphorylate Smad2 and regulate gene expression (Chen and Schier, 2001; Müller et al., 2012, 2013; Schier, 2003). Additionally, Nodal factors acquire their biological properties through maturation by proprotein convertases such as Furin (reviewed in Constam, 2014). In zebrafish, three different Nodal-related genes are known. Two of these, *squint (sqt)* and *cyclops (cyc),* are expressed during gastrulation and induce mesendoderm formation, while *southpaw* (*spaw*; and to a lesser extent *cyc)* are expressed in the left LPM and required for LR patterning (Long et al., 2003; Rebagliati et al., 1998). At early somatogenesis, *spaw* expression is initiated around the posteriorly localized Kupffer's vesicle, which is the functional homolog to the mouse's node, and is later enhanced in the left LPM due to cilia-mediated nodal flow, where it induces laterality of organs located posteriorly (e.g., gut) and anteriorly (e.g., heart and brain; see Long et al., 2003).

Making use of *ace of hearts (aoh)*, a zebrafish mutant for the proprotein convertase FurinA, we show that Spaw acquires its biological activity and signaling range via FurinA-mediated maturation. Our results point at a specific, cell-autonomous requirement of FurinA to process Spaw and the formation of an extracellular Spaw gradient. Our work demonstrates by in vivo experiments and in silico modeling that the level of FurinA expression in the zebrafish embryo controls the signaling range of Spaw, consequently acting as a regulator of LR asymmetry.

## RESULTS

### *aoh* Is a FurinA Mutant

The *aoh* mutant (Figure 1A) was identified in an *N*-ethyl-*N*-nitrosourea (ENU)-based forward genetic screen for mutants with organ laterality defects (Smith et al., 2011), as it displayed a midline-positioned cardiac tube at 28 hr postfertilization (hpf; Figure 1B). At 55 hpf, the heart of *aoh* mutants failed to undergo dextral looping and retained a linear tube morphology, although

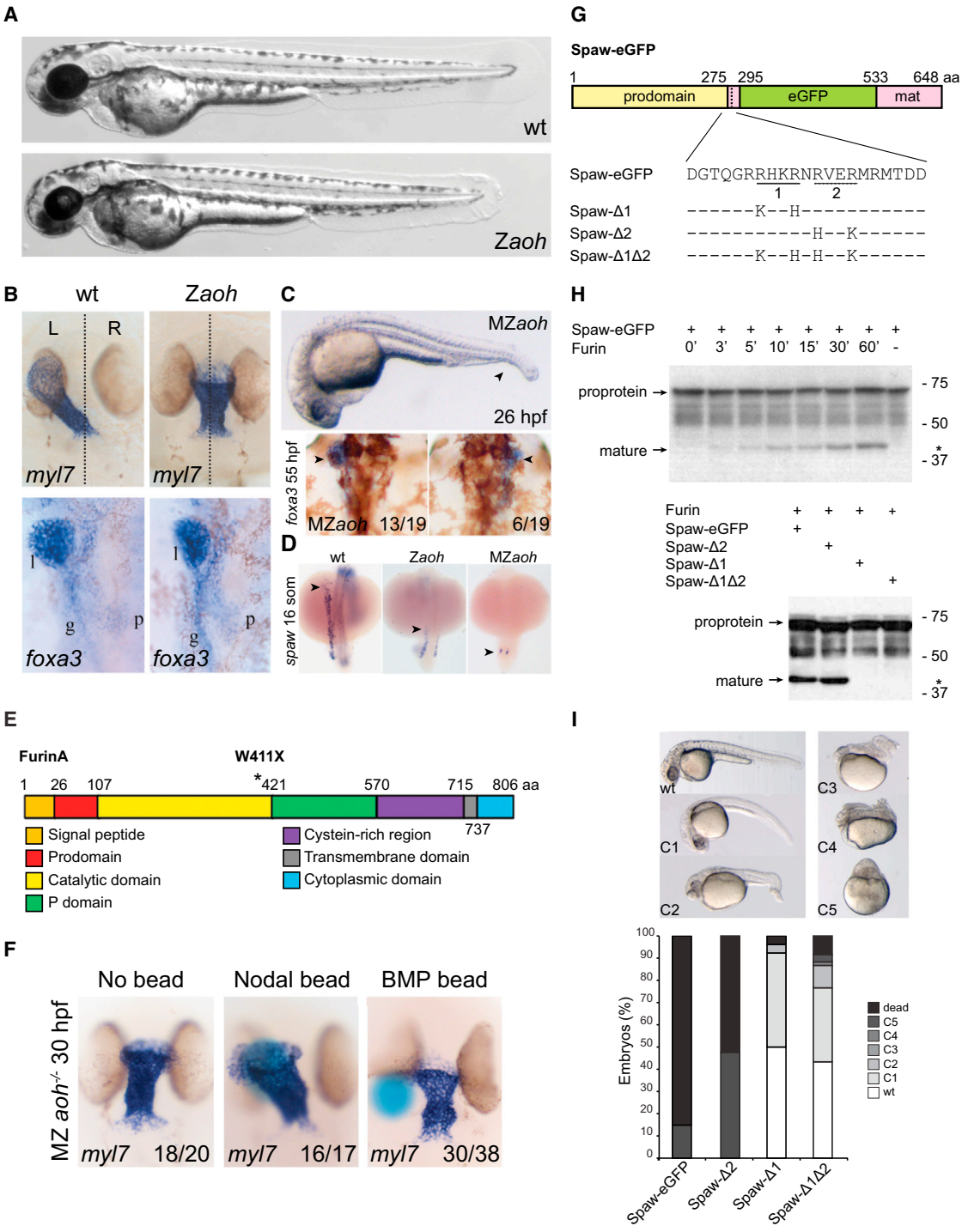


**Figure 1. Zygotic and Maternal Zygotic *aoh* Mutants Display Laterality Phenotypes and Defects in the Nodal Signaling Pathway**

(A) Lateral view of WT and *Zaoh* mutant embryos at 48 hpf.

(B) Characterization of the *Zaoh* mutant heart and gut phenotype. ISH at 28 hpf for *myl7* and at 55 hpf for *Foxa3* (dorsal view; anterior top).

(C) At 26 hpf, MZ*aoh* mutant embryos displayed slight developmental delay and a mild dorsalization phenotype in the tailfin (arrowhead). At 55 hpf, incidence of reversed gut looping and organ position was observed (arrowhead pointing at liver).

(D) ISH for *spaw* (arrowhead indicates anterior-ward expansion) in WT, *Zaoh*, and MZ*aoh* embryos.

(E) FurinA protein and functional domains. Star, *aoh* mutation.

(F) Agarose beads preincubated in recombinant BMP and Nodal protein were implanted in MZ*aoh* mutant embryos at 15 somites. Analysis of heart position was determined by *myl7* ISH.

*(legend continued on next page)*

all segments of the heart were properly specified (data not shown). The visceral organs were positioned correctly (Figure 1B). External observation of *aoh* at 55 hpf did not reveal any strong morphological defects, except for a mild shortening of the anterior-posterior axis and ruffling of the tail fin (Figure 1A). Although most *aoh* mutant embryos died due to failure to form a swim bladder, about 2% survived to adulthood. Maternal zygotic (MZ) *aoh* and zygotic (Z) *aoh* mutants appeared very similar except for a visible alteration in the tail fin of MZ*aoh* mutants (Figure 1C). While Z*aoh* and MZ*aoh* mutants displayed the same nonjogging cardiac phenotype, laterality of the visceral organs was only affected in MZ*aoh* mutants (Figure 1C), which was preceded by a complete loss of expression of the laterality marker genes *spaw* and *pitx2c* in the LPM (Figure 1D and Figure S1A available online). Using positional cloning, direct sequencing, and complementation testing, we determined that *aoh* mutants carry a point mutation resulting in a premature truncation of the FurinA subtilisin-like proprotein convertase (SPC; Figures 1E and S1B–S1D). Furin is part of a larger family of SPCs, which are crucial for conferring biological functionality to a wide variety of substrates including growth factors belonging to the Tgf-β superfamily (reviewed by Nakayama, 1997; Thomas, 2002). Furin-deficient mouse embryos die between embryonic day 10.5 (E10.5) and E11.5 and display various defects including a failure of ventral closure and axial rotation, as well as heart tube fusion and looping defects (Roebroek et al., 1998). To determine whether reduced Nodal signaling in *aoh* mutants is responsible for the cardiac laterality phenotype, we implanted agarose beads incubated with recombinant mature Nodal protein (Smith et al., 2008) in the left LPM of MZ*aoh* mutant embryos at 13–15 hpf and analyzed lateral displacement of the cardiac tube at 28 hpf. Nodal-soaked beads efficiently rescued the heart tube displacement defect in MZ*aoh* embryos (16/17 with leftward heart displacement; Figure 1F). To test the specificity of the rescue, we carried out a similar experiment using beads soaked in another Tgf-β family member important for LR patterning, namely Bmp, but these did not rescue the heart phenotype (Figure 1F).

## FurinA Processing Is Required for Spaw to Acquire Its Biological Properties

Since the laterality defects displayed by *aoh* mutants may be explained by reduced activity of Spaw, we first investigated whether Spaw can be cleaved by Furin. We identified two potential Furin cleavage sites (R-X-X-R) five amino acids from each other (Figure 1G; site 1 and site 2) in the sequence of the Spaw proprotein and inserted EGFP between site 2 and the Tgf-β domain (Figure 1G), allowing the fusion protein to retain its biological activity. Incubation of in vitro-translated Spaw-EGFP protein with recombinant Furin protein resulted in the efficient cleavage of Spaw-EGFP (Figure 1H). We also observed increased cleavage of Spaw-EGFP by FurinA in vivo in somatogenesis-stage mRNA-injected embryos (Figure S1F). To address whether any of the two potential Furin cleavage sites identified in Spaw are essential to this process, we mutated each site individually or together (Figure 1G). When we incubated in vitro-translated products of the Spaw-EGFP variants with recombinant Furin, we could establish that only the more upstream (site 1; R-H-K-R) of the two potential sites is efficiently cleaved by Furin (Figure 1H). To assess whether cleavage by Furin affects the biological activity of Spaw in vivo, we overexpressed the different Spaw-EGFP fusion variants in zebrafish embryos and scored for dorsalization phenotypes induced by ectopic Nodal signaling (Gritsman et al., 1999; Kishimoto et al., 1997; Mullins et al., 1996; Noël et al., 2013). Spaw-EGFP variants that retained the ability to be cleaved by Furin (Spaw-EGFP and Spaw-Δ2; Figure 1H) induced strong dorsalization or death (Figure 1I). On the contrary, Furin-resistant Spaw-Δ1 and Spaw-Δ1Δ2 were compromised in their ability to dorsalize the embryo (Figure 1I). Thus, cleavage by Furin promotes the biological activity of Spaw.

We previously showed that Spaw activity in the LPM is required to maintain *spaw* expression thanks to a positive feedback loop (Noël et al., 2013). To address whether in the LPM Spaw acts only on cells adjacent or also on cells located at a larger distance from the Spaw source, we performed transplantation experiments (Figure 2A) in maternal and zygotic *sfw/spaw* mutant embryos, which lack functional Spaw protein (see Noël et al., 2013; Figures 2B, 2D, 2E, and 2G). While *sfw/spaw* mutants lack endogenous *spaw* expression in the anterior LPM, robust unilateral *spaw* expression was restored when donor cells derived from embryos injected with *spaw* mRNA were transplanted to the LPM of *sfw/spaw* mutants (18/38 transplants; Figure 2D). We observed induction of endogenous *spaw* expression several cell diameters away from the transplanted clones (Figure 2D). Since functional Spaw is only expressed in the transplanted cells, this indicates that Spaw has long-range signaling activity within the LPM. This observation is not restricted to zebrafish Spaw, since mouse recombinant mature Nodal protein, when delivered in the LPM of *sfw/spaw* mutant embryos, also displayed long-range signaling activity (Figure S2). To address whether processing of Spaw by SPCs is required for the observed long-range signaling activity, we expressed Furin-resistant Spaw-Δ1 in the transplanted clones (Figure 2E). We observed that Furin-resistant Spaw-Δ1 was not able to induce endogenous *spaw* expression outside the transplanted clone in the LPM (34/34 transplants; Figure 2E). This suggests that processing of Spaw by FurinA is required for either, (1) the formation of a mature Spaw gradient in the extracellular environment, or (2) activation of Nodal signaling in the receiving cell.

In vitro and in vivo experiments in early mouse embryos suggested that Furin-like SPCs could act noncell autonomously and process Nodal extracellularly to allow induction of Nodal signaling in the receiving cell (Beck et al., 2002; Blanchet et al., 2008; Mesnard et al., 2011). Surprisingly, we observed that transplanted cell clones derived from MZ*aoh* mutant donor embryos injected with *spaw* mRNA failed to induce endogenous *spaw* expression in the LPM of *sfw/spaw* mutant recipients (85/85 transplants; Figure 2G), demonstrating that Furin is

(G and H) Spaw-EGFP fusion protein (G). Furin recognition sites 1 and 2 are underlined. Changes in amino acids in the noncleavable forms are detailed (H) western blot with anti-GFP. Incubation of Spaw with Furin results in cleavage and appearance of the mature 41 kDa Spaw-EGFP (asterisk). Incubation of the different Spaw-EGFP variants with Furin demonstrates that cleavage happens only at the single (optimal) predicted Furin cleavage site 1.
(I) Dorsalization phenotypes induced by injection of Spaw-EGFP variants mRNA (1 picogram [pg]) at 24 hpf. Abbreviations, liver (l), pancreas (p), and gut (g).

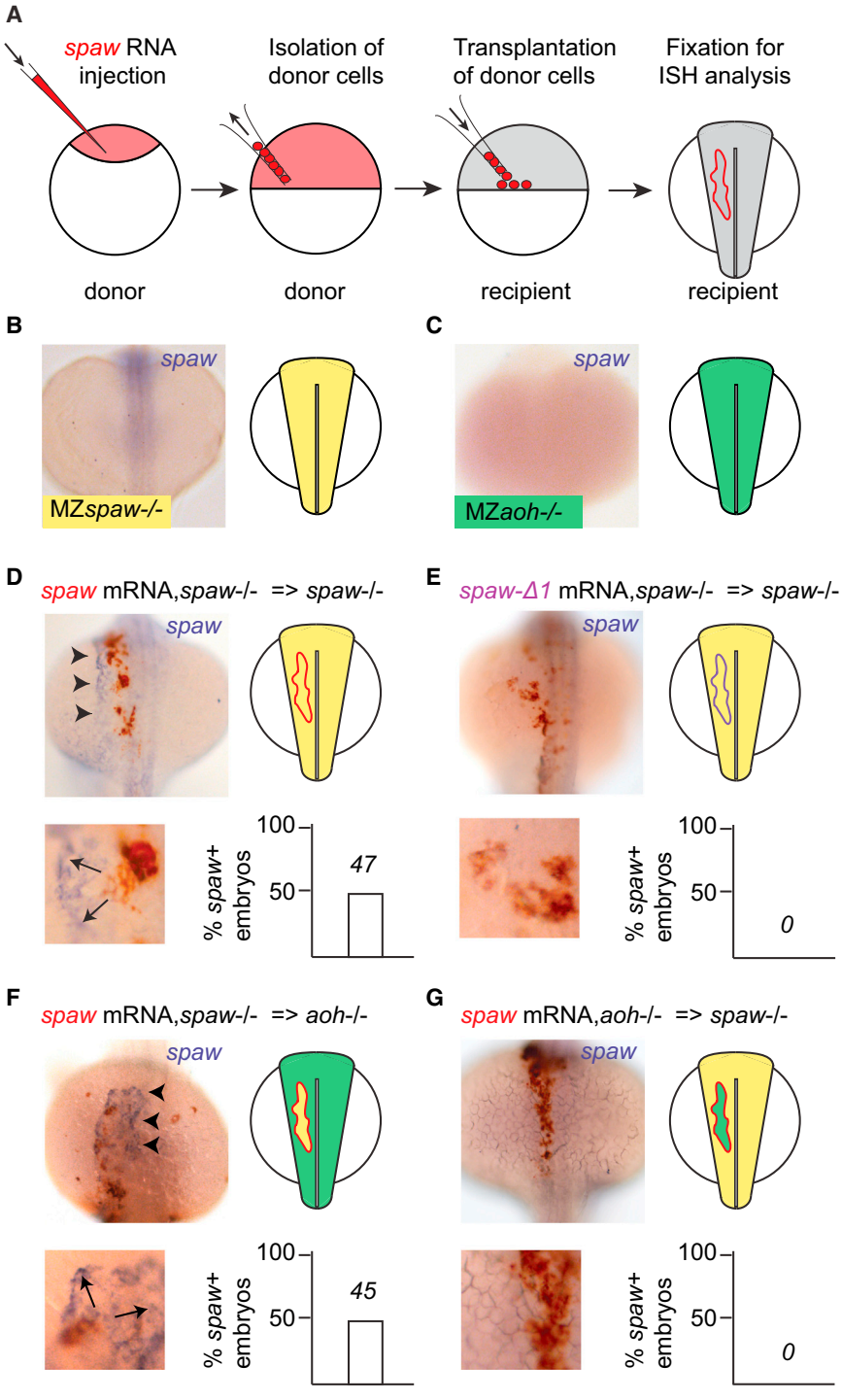


**Figure 2. FurinA Is Required Cell-Autonomously to Process Spaw and to Confer Its Long-Range Signaling Activity**

(A) Schematic of the transplantation procedure.

(B and C) Both MZ*spaw*$^{-/-}$ (B) and MZ*aoh*$^{-/-}$ (C) embryos fail to express *spaw* in the left LPM at 18 somites.

(D) ISH for *spaw* (blue staining) with immunolabeling for transplanted cells (red staining). Transplantation of *spaw*-injected *spaw*$^{-/-}$ cells (yellow clone, red outline) in MZ*spaw*$^{-/-}$ resulted in the rescue of *spaw* expression in the left LPM several cell diameters away from the transplanted clone.

(E) Transplantation of cells injected with RNA of a noncleavable form of *spaw* (yellow clone, purple outline) in MZ*spaw*$^{-/-}$ failed to induce of *spaw* expression in the left LPM.

(F) Transplantation of *spaw*-injected spaw$^{-/-}$ cells (yellow clone, red outline) in MZ*aoh*$^{-/-}$ resulted in induction of *spaw* expression in the left LPM several cell diameters away from the transplanted clone.

(G) *Spaw*-injected *aoh*$^{-/-}$ cells (green clone, red outline) in MZ*spaw*$^{-/-}$ were unable to induce *spaw* expression in the left LPM. In all schematics, MZ*spaw*$^{-/-}$ cells appear in yellow and MZ*aoh*$^{-/-}$ cells in green.

required cell-autonomously in the LPM. We also performed the reverse experiment by transplanting cell clones derived from *sfw/spaw* embryos injected with *spaw* mRNA in the LPM of MZ*aoh* mutant embryos. While MZ*aoh* mutant embryos are devoid of endogenous *spaw* expression in the anterior LPM (Figure 2C), *sfw/spaw* clones overexpressing *spaw* mRNA efficiently induced endogenous *spaw* expression in the anterior LPM of MZ*aoh* mutant recipients (5/11 transplants; Figure 2F), confirming a strict cell-autonomous requirement for Furin. Together, these results demonstrate not only that Spaw has long-range signaling activity in the LPM, but also that this requires cell-autonomous FurinA activity in the Spaw-producing cells.

## FurinA-Mediated Processing of Spaw Correlates Specifically with Spaw Localization to the Extracellular Space

To assess how FurinA affects Spaw activity, we visualized Spaw-EGFP localization in blastula stage embryos. Surprisingly, Spaw-EGFP was predominantly localized intracellularly (Figure 3A; 7/9 embryos) and was converted in a mostly extracellular localization when *furina* mRNA was coinjected (Figure 3A; 13/15 embryos), suggesting that FurinA-mediated maturation correlates positively with extracellular Spaw localization. Corroborating this hypothesis, we observed that the cleavage-deficient Spaw-Δ1, which predominantly displays intracellular localization (Figure 3A; 11/13 embryos), was not localizing efficiently in the extracellular space even when *furina* RNA was coinjected (Figure 3A; 6/11 embryos). In agreement with this result, we observed extracellular Spaw-EGFP localization in the LPM of wild-type, but not of *Zaoh* late somite-stage embryos (Figure S3A). Interestingly, the ability of Spaw to be processed also correlated positively with its capacity to induce *no tail,* an early Nodal target gene, at a distance of numerous cell

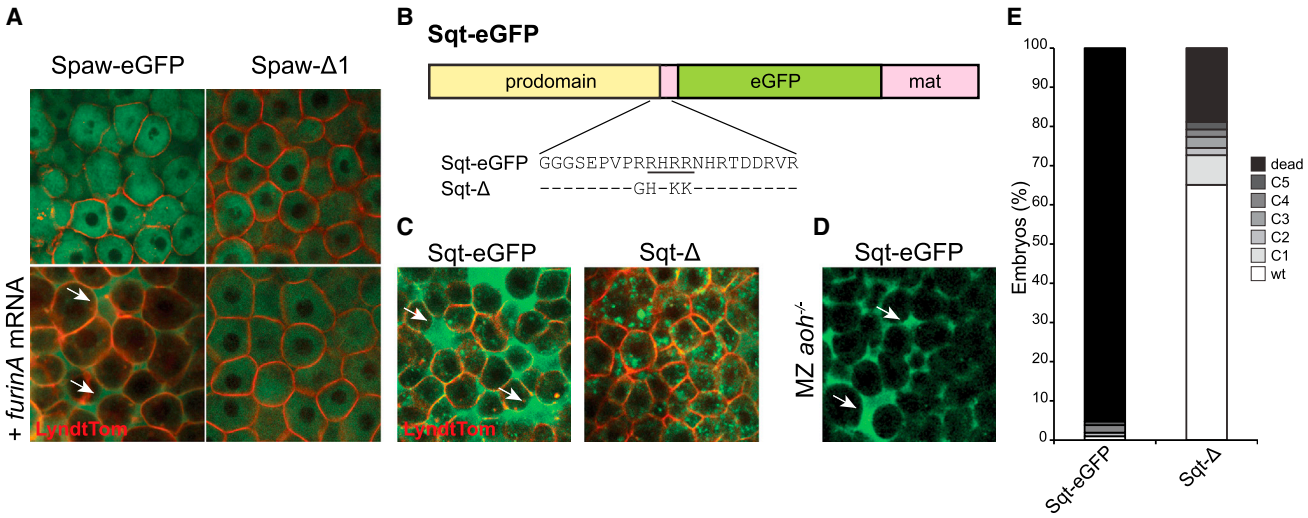


**Figure 3. FurinA-Mediated Processing of Spaw Specifically Correlates with Extracellular Localization of Spaw**

(A) Embryos were injected at the one-cell stage with 50 pg of Spaw-EGFP mRNA or Spaw-Δ1 mRNA together with a membrane-bound tdTomato fusion protein and imaged at sphere stage (4 hpf). Addition of FurinA mRNA (30 pg) to the injection mix resulted in an increased extracellular localization of Spaw-EGFP, but not Spaw-Δ1.

(B) Schematic representation of the Sqt-EGFP fusion protein (Müller et al., 2012). The Furin recognition site is underlined in the detail of the sequence. The changes in amino acids in the noncleavable form Sqt-Δ are detailed.

(C) Removal of the Furin cleavage site (Sqt-Δ) resulted in reduced extracellular localization of Sqt-EGFP. mRNA injections and imaging were carried out identically to (A).

(D) MZ*aoh* mutant embryos were injected at the one-cell stage with 50 pg Sqt-EGFP mRNA and imaged at sphere stage (4 hpf). Arrows indicate extracellular localization of the Spaw-EGFP and Sqt-EGFP fusion proteins respectively in (A), (C), and (D).

(E) Quantification of the dorsalization phenotypes induced by injection of 1 pg Sqt-EGFP and Sqt-Δ. The embryos were scored as described in Figure 1I.

diameters in blastula stage embryos (Figures S3B–S3D); (Chen and Schier, 2001; Jing et al., 2006; Müller et al., 2012; Tian et al., 2008). Previous work has shown that Squint-EGFP (Figure 3B), another zebrafish Nodal-related factor with long-range signaling activity, is localized mainly extracellularly (Chen and Schier, 2001; Müller et al., 2012). We confirmed the extracellular localization of Squint-EGFP without coinjection of *furina* mRNA, suggesting that Spaw, and not Squint, requires FurinA for efficient extracellular localization (Figure 3C). Accordingly, Squint-EGFP localized normally in MZ*aoh* mutant embryos, which are devoid of FurinA (Figure 3D), confirming that Squint processing and extracellular localization are FurinA-independent. Interestingly, mutating the single potential SPC cleavage site present in Squint-EGFP compromised both its extracellular localization and its biological activity (Figures 3C and 3E), suggesting that an SPC other than FurinA is required for the efficient maturation and extracellular localization of Squint. Supporting this conclusion, we never observed defects in mesendoderm induction (Feldman et al., 1998; Thisse et al., 1994) in *Zaoh* or MZ*aoh* mutants. Together, these results demonstrate that the FurinA-mediated cleavage of Spaw is required for the formation of the extracellular Spaw gradient. Additionally, our data highlight the high level of specificity underlying the processing of Nodal-related proteins by SPCs.

## FurinA Expression Levels Control LR Asymmetry via Regulation of Spaw Signaling Range

It has been proposed that mouse Nodal is secreted as a proprotein and cleaved by SPCs extracellularly (Beck et al., 2002; Blanchet et al., 2008). Our results challenge this model for the Nodal-related Spaw factor, as they demonstrate not only that FurinA is required cell-autonomously in the Spaw-producing cells, but also that FurinA processing controls the formation of the Spaw extracellular gradient. To understand how FurinA processing of Spaw controls the establishment of the Nodal signaling domain in the LPM during LR patterning, we developed a mathematical model (Figure 4; the mathematical equations are shown in Figure 4C and detailed in the Supplemental Experimental Procedures). In brief, in this one-dimension reaction-diffusion model (Figures 4A and 4B), the maturation of Spaw is controlled by FurinA processing. Once processed, Spaw is secreted and forms an extracellular gradient. Extracellular mature Spaw diffuses to surrounding cells, where it binds to its receptor and stimulates the production of intracellular Spaw. Both intracellular and extracellular Spaw are assumed to be degraded according to first order kinetics, i.e., due to proteolysis independent of Spaw or FurinA. Most importantly, this model produces a front of extracellular, mature Spaw protruding into the LPM, with a propagation speed that is enhanced by the level of FurinA. In Movie S1, snapshots of which are shown in Figure 4D, the faster propagation of extracellular Spaw resulting from an increase in FurinA levels can be appreciated. The mathematical model predicts that the distance reached by a specific amount of extracellular Spaw within a given time is a function of FurinA levels (Figure 4E). Due to its self-inducing activity, we used the *spaw* expression domain as a readout for extracellular Spaw activity in vivo. With increasing FurinA levels, the model predicts an increasing anterior extension of the *spaw* expression domain

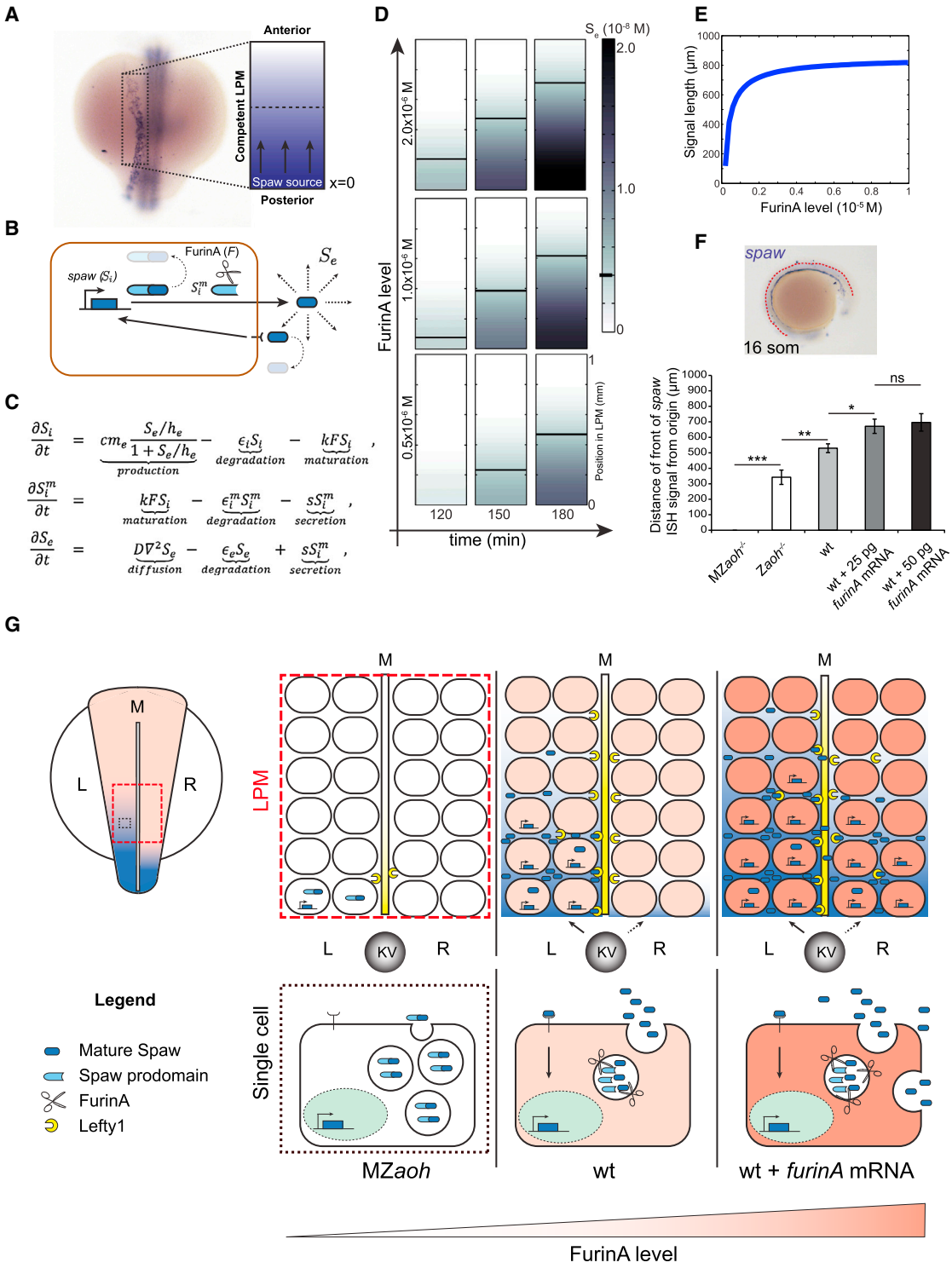


**Figure 4. FurinA Levels Control the Expansion of the Spaw Expression Domain in the LPM**

(A and B) For the purpose of mathematical modeling, we have considered the left LPM of the developing zebrafish embryo as a linear domain (displayed as a rectangle here) with a source of Spaw at the posterior end ($x = 0$); (B) behavior of Spaw in the competent LPM described in (A). Synthetized intracellular Spaw ($S_i$), mature intracellular Spaw ($S_i^m$), and extracellular Spaw ($S_e$).

(C) Partial-differential equation model of the system described in (B). Parameter definitions, analysis of the model, and details on the numerical simulation and boundary conditions are available in Supplemental Experimental Procedures.

(D) Snapshots of Movie S1 showing a simulation of the model defined in (C). The speed of progression of $S_e$, and consequently of the domain of *spaw* expression in the LPM, increases with the level of FurinA.

*(legend continued on next page)*

at a given developmental stage. To test this prediction in vivo, we determined the signaling range of Spaw in the LPM by measuring the length of the *spaw* expression domain in embryos with different levels of FurinA (Figure 4F). First, we compared the *spaw* expression domain in embryos with no FurinA (MZ*aoh* mutant), low levels of FurinA (*Zaoh*), and normal FurinA expression (wild-type [WT] embryos). In agreement with the prediction of the mathematical model, we observed that the *spaw* expression domain in the LPM was absent in the MZ*aoh* mutant embryos, while the extension of the *spaw* expression domain was limited in *Zaoh* mutant embryos, which is consistent with its expression in the posterior, but not in the anterior LPM (Figures 1D and S1A). Additionally, we tested the expression of Nodal-dependent genes in MZ*aoh* and *Zaoh* mutants to confirm the suggested difference in the signaling range of Spaw. We observed that Nodal-dependent expression of *lefty1, lefty2*, and *pitx2c* was lost in MZ*aoh* mutant embryos, while their expression was maintained in the posterior region, but not in the anterior region of *Zaoh* mutant embryos (Figure S1A). Consequently, in *Zaoh* mutants, laterality of posterior organs such as gut, liver, and pancreas was unaffected, while laterality of anterior organs (e.g., heart) was affected resembling *situs ambiguus* or heterotaxia (discordance between organ laterality; Figures 1 and S1).

Next, we examined whether increasing FurinA levels in WT embryos would be sufficient to expand the signaling range of Spaw even further in the anterior direction, as the mathematical model predicts. Since endogenous *furina* is broadly expressed at early developmental stages and during somitogenesis (Figure S1E; see Walker et al., 2006), we overexpressed FurinA in all cells by mRNA injection into WT embryos and determined the anterior-posterior length of the *spaw* expression domain. We observed that increasing FurinA was sufficient to induce an anterior-ward expansion of the signaling range of Spaw (Figure 4F). Interestingly, increased FurinA expression levels resulted not only in faster expansion of *spaw* expression toward the anterior LPM, but also in an increased incidence of bilateral *spaw* expression and the appearance of right-sided *spaw* expression in the LPM (Figure S4). This could be the consequence of the saturation of the midline barrier and of the activity of a self-enhancement lateral-inhibition system, as described for mouse Nodal and Lefty (see model in Figure 4F; see Nakamura et al., 2006). Altogether, we conclude that the level of FurinA determines the signaling range of Spaw in the LPM, which is critical for the establishment of correct LR patterning of the embryo.

## DISCUSSION

We conclude that FurinA can cleave the Nodal-related Spaw proprotein into a prodomain and a mature, biologically active growth factor. Maturation by FurinA thus facilitates the efficient formation of an extracellular Spaw gradient and is required for its long-range signaling activity (Figure 4G). Expression of *spaw* is initiated in the posterior LPM by a thus far unknown mechanism. Due to a positive feedback mechanism, *spaw* expression expands in the anterior direction. FurinA-mediated maturation of Spaw regulates the speed at which this expression domain expands in the anterior direction, which is essential for correct establishment of LR patterning and organ laterality. In our model, the heart is more sensitive to altered extracellular Nodal levels or Nodal signaling activity than the abdominal organs are. Therefore, the proposed model provides a good explanation for the occurrence of heterotaxia syndrome, which is often associated with complex congenital heart or lung defects, and the occurrence of isolated congenital heart defects that are very similar to those observed in heterotaxia syndrome (e.g., transposition of the great arteries or double outlet right ventricle; reviewed in Ramsdell, 2005). Indeed, a patient with a dextro-transposition of the great arteries and a normal laterality of abdominal organs was reported with an insertion and in frame deletion affecting the SPC cleavage site in NODAL (Mohapatra et al., 2009). In addition, genome-wide association studies have pointed toward a common variant located in an intron of the proprotein convertase PCSK6 to be related to brain organization and handedness in humans (Brandler et al., 2013; Scerri et al., 2011).

Additionally to demonstrating how FurinA acts as a regulator of LR patterning by controlling the signaling range of Spaw, our work suggests a further mechanism for the formation of exponential gradients: synthesis, controlled maturation, and relay of synthesis to the next cell. An interesting aspect of this model is that maturation of Spaw by FurinA controls the extension speed. Furthermore, our data demonstrate a high specificity between Nodal-related factors and protein convertases, which is illustrated by the absence of mesendoderm specification defects, typical of early Nodal deficiency, in *Zaoh* and MZ*aoh* mutants.

## EXPERIMENTAL PROCEDURES

### Fish Lines and Husbandry

The zebrafish lines used in this study were: *sfw/spaw* (Noël et al., 2013), stu/*furina*$^{td204e}$ (Walker et al., 2006), tg(hsp70:Gal4; see Scheer et al., 2001), and

(E) The model predicted that increasing FurinA levels, resulting in enhanced maturation of Spaw, results in increased length of the *spaw* expression domain at a given time (180 min here).

(F) Quantification of the length of the *spaw* expression domain (anterior-posterior) in embryos with no (MZ*aoh*; n = 12), low (*Zaoh* mutants; n = 7), normal (WT; n = 15), or high (WT injected respectively with 25 pg; n = 25 and 50 pg; n = 17 *furina* mRNA) FurinA levels. Histograms display average value ± SEM; *p < 0.05, **p < 0.01, and ***p < 0.005 in Student's t test.

(G) Cartoon illustrating the effect of FurinA on the signaling range of Spaw in the LPM. In a WT situation, Spaw is cleaved prior to secretion by cells at the posterior end of the LPM (10 somite stage, 13 hpf). Spaw induces its own expression in a paracrine fashion, and the *spaw* expression domain expands toward the anterior end of the developing LPM, reaching the heart field at the 23-somite stage (20 hpf). Spaw also induces expression of Lft1 at the midline, which prevents it from reaching the right LPM. Spaw expression is consequently limited to the left LPM and establishes LR patterning. In the MZ*aoh* mutants, the absence of FurinA processing of Spaw results in failure to induce Spaw expression in the LPM and of Lft1 in the midline. As a consequence, LR patterning is affected. Overexpression of FurinA results in increased presence of mature Spaw in the extracellular space. The activation of Spaw in the LPM progresses faster toward the anterior left LPM. LR patterning is affected, likely as a result of an excess of Spaw protein overcoming the Lft1 midline barrier, Kupffer's Vesicle (KV) and midline (M).

Tübingen longfin. Fish were kept under standard conditions. The ENU mutagenesis screen was performed as described in Wienholds et al. (2003). Animal experiments were approved by the Animal Experimentation Committee of the Royal Netherlands Academy of Arts and Sciences.

### Positional Cloning of *aoh*

The *aoh/furina*$^{hu119}$ allele was mapped using standard meiotic mapping with simple sequence length polymorphisms (SSLPs). SSLP primer sequences located in the region ca1–ca3 (Figure S2) can be found in the Supplemental Experimental Procedures. The *aoh/furina*$^{hu119}$ mutation is identified by PCR amplification from genomic DNA using primers FT207: 50-CCTCACATTTGAAGGCCACT-30 (forward) and FT208-rev: 50-CGCCACAAAACGTTCAAGTA-30 and followed by BfaI restriction of the PCR product. The *aoh/furina*$^{hu119}$ mutation introduces a BfaI restriction site.

### In Situ Hybridization

In situ hybridization was essentially carried out as previously described (Noël et al., 2013). The succinct protocol can be found in the Supplemental Experimental Procedures.

### Generation of Fluorescent and Cleavage-Resistant Spaw and Squint Variants

The EGFP sequence was introduced 14 amino acids downstream of Furin cleavage site 2 (**RVER**), between the prodomain and the mature domain of Spaw in spaw-pCS2+ (Noël et al., 2013), generating spaw-EGFP-pCS2+. The Δ1 and Δ2 mutations were by site-directed mutagenesis using a Quikchange Kit (Stratagene Europe). Squint-Δ was obtained similarly using as template PCS2-Squint-GFP (Müller et al., 2012). Accession numbers are *spaw* (NM_180967) and *squint* (NM_130966).

### mRNA Injections

mRNA for injections was transcribed using the SP6 mMessage mMachine Kit (Life Technologies BV) using as a template linearized PCS2+ constructs for all genes. Embryos were injected at the one-cell stage with various concentrations of mRNA depending on the experiment performed.

### In Vitro Protein Synthesis and Western Blotting

In vitro protein synthesis was carried out using the TnT SP6 High-Yield Wheat Germ Protein Expression System (Promega) following the manufacturer's protocol. Furin cleavage assays were carried out using recombinant human Furin (Sigma-Aldrich) as described in Molloy et al. (1992). Samples were run on a 10% acrylamide gel in Laemmli buffer and western blotting was carried out with 1:4,000 rabbit-anti-GFP (#TP401; Torrey Pines Biolabs) and 1:5,000 anti-rabbit-HRP antibody (#NA934; GE Healthcare). Detection was carried out with a SuperSignal West Pico ECL System (Thermo Fisher Scientific).

### Bead Implants

Bead implants were carried out as previously described (Smith et al., 2008, 2011), with minor modifications.

### Transplantations

For assaying induction of *spaw* expression at somitogenesis, donor embryos were injected at the one-cell stage with approximately 1 nanoliter mRNA of spaw, spaw-EGFP, spaw-Δ1, spaw-Δ2, spaw-Δ1Δ2 (all 10 ng/μl) with 2 μg/μl 2,000 KDa Fluorescein isothiocyanate–dextran (Sigma-Aldrich), and left to develop at 28.5°C. At dome stage, embryos were transferred to E3 medium supplemented with Penicillin/Streptomycin (Life Technologies). Around 50 cells were transplanted from donor embryos into the margin of recipient embryos at shield stage with an Eppendorf Celltram Vario Microinjector (Eppendorf). Embryos were subsequently left to grow until the 18 somites stage and fixed in 4% paraformaldehyde. In situ hybridization (ISH) with the *spaw* RNA probe was carried out as described above. Fluorescein in the donor clone cells was detected using an anti-fluorescein antibody in combination with a 2-(4-iodophenyl)-5-(4-nitrophenyl)-3-phenyltetrazolium chloride/5-bromo-4-chloro-3-inodyl phosphate substrate (Roche).

## SUPPLEMENTAL INFORMATION

Supplemental Information includes Supplemental Experimental Procedures, four figures, and one movie and can be found with this article online at http://dx.doi.org/10.1016/j.devcel.2014.12.014.

## AUTHOR CONTRIBUTIONS

F.T., E.S.N., E.G.R., D.G., R.M.H.M., and J.B. designed the experiments. R.M. and D.G. provided reagents. F.T., E.S.N., E.G.R., R.M., and I.J.A.E.-v.G. collected data. F.T., E.S.N., E.G.R., D.G., R.M.H.M., and J.B. analyzed and interpreted the data. F.T., E.G.R., R.M.H.M., and J.B. wrote and revised the manuscript.

## ACKNOWLEDGMENTS

We thank Rik Korswagen for critical reading of the manuscript, members of the Bakkers' Laboratory for their suggestions, and the Hubrecht Imaging Center. The pCS2-Squint-GFP is a gift of A. Schier (Harvard University, Cambridge, MA, USA). The pCS2-LynTdTomato plasmid was obtained from V. Lecaudey (University of Freiburg, Freiburg, Germany). The investigations were supported by the Division for Earth and Life Sciences, with financial aid from the Netherlands Organisation for Scientific Research.

Received: July 10, 2014
Revised: October 29, 2014
Accepted: December 17, 2014
Published: February 12, 2015

## REFERENCES

Beck, S., Le Good, J.A., Guzman, M., Ben Haim, N., Roy, K., Beermann, F., and Constam, D.B. (2002). Extraembryonic proteases regulate Nodal signalling during gastrulation. Nat. Cell Biol. *4*, 981–985.

Blanchet, M.H., Le Good, J.A., Mesnard, D., Oorschot, V., Baflast, S., Minchiotti, G., Klumperman, J., and Constam, D.B. (2008). Cripto recruits Furin and PACE4 and controls Nodal trafficking during proteolytic maturation. EMBO J. *27*, 2580–2591.

Brandler, W.M., Morris, A.P., Evans, D.M., Scerri, T.S., Kemp, J.P., Timpson, N.J., St Pourcain, B., Smith, G.D., Ring, S.M., Stein, J., et al. (2013). Common variants in left/right asymmetry genes and pathways are associated with relative hand skill. PLoS Genet. *9*, e1003751.

Chen, Y., and Schier, A.F. (2001). The zebrafish Nodal signal Squint functions as a morphogen. Nature *411*, 607–610.

Constam, D.B. (2014). Regulation of TGFβ and related signals by precursor processing. Semin. Cell Dev. Biol. *32*, 85–97.

Driever, W., and Nüsslein-Volhard, C. (1988). A gradient of bicoid protein in Drosophila embryos. Cell *54*, 83–93.

Feldman, B., Gates, M.A., Egan, E.S., Dougan, S.T., Rennebeck, G., Sirotkin, H.I., Schier, A.F., and Talbot, W.S. (1998). Zebrafish organizer development and germ-layer formation require nodal-related signals. Nature *395*, 181–185.

Gritsman, K., Zhang, J., Cheng, S., Heckscher, E., Talbot, W.S., and Schier, A.F. (1999). The EGF-CFC protein one-eyed pinhead is essential for nodal signaling. Cell *97*, 121–132.

Jing, X.H., Zhou, S.M., Wang, W.Q., and Chen, Y. (2006). Mechanisms underlying long- and short-range nodal signaling in Zebrafish. Mech. Dev. *123*, 388–394.

Kishimoto, Y., Lee, K.H., Zon, L., Hammerschmidt, M., and Schulte-Merker, S. (1997). The molecular nature of zebrafish swirl: BMP2 function is essential during early dorsoventral patterning. Development *124*, 4457–4466.

Long, S., Ahmad, N., and Rebagliati, M. (2003). The zebrafish nodal-related gene southpaw is required for visceral and diencephalic left-right asymmetry. Development *130*, 2303–2316.

Mesnard, D., Donnison, M., Fuerer, C., Pfeffer, P.L., and Constam, D.B. (2011). The microenvironment patterns the pluripotent mouse epiblast through paracrine Furin and Pace4 proteolytic activities. Genes Dev. *25*, 1871–1880.

Mohapatra, B., Casey, B., Li, H., Ho-Dawson, T., Smith, L., Fernbach, S.D., Molinari, L., Niesh, S.R., Jefferies, J.L., Craigen, W.J., et al. (2009). Identification and functional characterization of NODAL rare variants in heterotaxy and isolated cardiovascular malformations. Hum. Mol. Genet. *18*, 861–871.

Molloy, S.S., Bresnahan, P.A., Leppla, S.H., Klimpel, K.R., and Thomas, G. (1992). Human furin is a calcium-dependent serine endoprotease that recognizes the sequence Arg-X-X-Arg and efficiently cleaves anthrax toxin protective antigen. J. Biol. Chem. *267*, 16396–16402.

Müller, P., Rogers, K.W., Jordan, B.M., Lee, J.S., Robson, D., Ramanathan, S., and Schier, A.F. (2012). Differential diffusivity of Nodal and Lefty underlies a reaction-diffusion patterning system. Science *336*, 721–724.

Müller, P., Rogers, K.W., Yu, S.R., Brand, M., and Schier, A.F. (2013). Morphogen transport. Development *140*, 1621–1638.

Mullins, M.C., Hammerschmidt, M., Kane, D.A., Odenthal, J., Brand, M., van Eeden, F.J., Furutani-Seiki, M., Granato, M., Haffter, P., Heisenberg, C.P., et al. (1996). Genes establishing dorsoventral pattern formation in the zebrafish embryo: the ventral specifying genes. Development *123*, 81–93.

Nakamura, T., Mine, N., Nakaguchi, E., Mochizuki, A., Yamamoto, M., Yashiro, K., Meno, C., and Hamada, H. (2006). Generation of robust left-right asymmetry in the mouse embryo requires a self-enhancement and lateral-inhibition system. Dev. Cell *11*, 495–504.

Nakayama, K. (1997). Furin: a mammalian subtilisin/Kex2p-like endoprotease involved in processing of a wide variety of precursor proteins. Biochem. J. *327*, 625–635.

Noël, E.S., Verhoeven, M., Lagendijk, A.K., Tessadori, F., Smith, K., Choorapoikayil, S., den Hertog, J., and Bakkers, J. (2013). A Nodal-independent and tissue-intrinsic mechanism controls heart-looping chirality. Nat. Commun. *4*, 2754.

Ramsdell, A.F. (2005). Left-right asymmetry and congenital cardiac defects: getting to the heart of the matter in vertebrate left-right axis determination. Dev. Biol. *288*, 1–20.

Rebagliati, M.R., Toyama, R., Fricke, C., Haffter, P., and Dawid, I.B. (1998). Zebrafish nodal-related genes are implicated in axial patterning and establishing left-right asymmetry. Dev. Biol. *199*, 261–272.

Roebroek, A.J., Umans, L., Pauli, I.G., Robertson, E.J., van Leuven, F., Van de Ven, W.J., and Constam, D.B. (1998). Failure of ventral closure and axial rotation in embryos lacking the proprotein convertase Furin. Development *125*, 4863–4876.

Scerri, T.S., Brandler, W.M., Paracchini, S., Morris, A.P., Ring, S.M., Richardson, A.J., Talcott, J.B., Stein, J., and Monaco, A.P. (2011). PCSK6 is associated with handedness in individuals with dyslexia. Hum. Mol. Genet. *20*, 608–614.

Scheer, N., Groth, A., Hans, S., and Campos-Ortega, J.A. (2001). An instructive function for Notch in promoting gliogenesis in the zebrafish retina. Development *128*, 1099–1107.

Schier, A.F. (2003). Nodal signaling in vertebrate development. Annu. Rev. Cell Dev. Biol. *19*, 589–621.

Schier, A.F. (2009). Nodal morphogens. Cold Spring Harb. Perspect. Biol. *1*, a003459.

Shiratori, H., and Hamada, H. (2006). The left-right axis in the mouse: from origin to morphology. Development *133*, 2095–2104.

Smith, K.A., Chocron, S., von der Hardt, S., de Pater, E., Soufan, A., Bussmann, J., Schulte-Merker, S., Hammerschmidt, M., and Bakkers, J. (2008). Rotation and asymmetric development of the zebrafish heart requires directed migration of cardiac progenitor cells. Dev. Cell *14*, 287–297.

Smith, K.A., Noël, E., Thurlings, I., Rehmann, H., Chocron, S., and Bakkers, J. (2011). Bmp and nodal independently regulate lefty1 expression to maintain unilateral nodal activity during left-right axis specification in zebrafish. PLoS Genet. *7*, e1002289.

Thisse, C., Thisse, B., Halpern, M.E., and Postlethwait, J.H. (1994). Goosecoid expression in neurectoderm and mesendoderm is disrupted in zebrafish cyclops gastrulas. Dev. Biol. *164*, 420–429.

Thomas, G. (2002). Furin at the cutting edge: from protein traffic to embryogenesis and disease. Nat. Rev. Mol. Cell Biol. *3*, 753–766.

Tian, J., Andrée, B., Jones, C.M., and Sampath, K. (2008). The pro-domain of the zebrafish Nodal-related protein Cyclops regulates its signaling activities. Development *135*, 2649–2658.

Walker, M.B., Miller, C.T., Coffin Talbot, J., Stock, D.W., and Kimmel, C.B. (2006). Zebrafish furin mutants reveal intricacies in regulating Endothelin1 signaling in craniofacial patterning. Dev. Biol. *295*, 194–205.

Wartlick, O., Kicheva, A., and González-Gaitán, M. (2009). Morphogen gradient formation. Cold Spring Harb. Perspect. Biol. *1*, a001255.

Wienholds, E., van Eeden, F., Kosters, M., Mudde, J., Plasterk, R.H., and Cuppen, E. (2003). Efficient target-selected mutagenesis in zebrafish. Genome Res. *13*, 2700–2707.